Supplementary Information

Ultrasoft, Elastic, and Ionically Conductive Polyethylene Glycol/Ionic Liquid Bottlebrush Ionogels

Pengfei Xu, Siddhartha Challa, Zefang Zhang, Xia Wu, Shaojia Wang, Peng Pan, Xinyu Liu**

This PDF file includes:

Supplementary Figs. S1 to S17

Supplementary Tables S1 to S3

Supplementary References

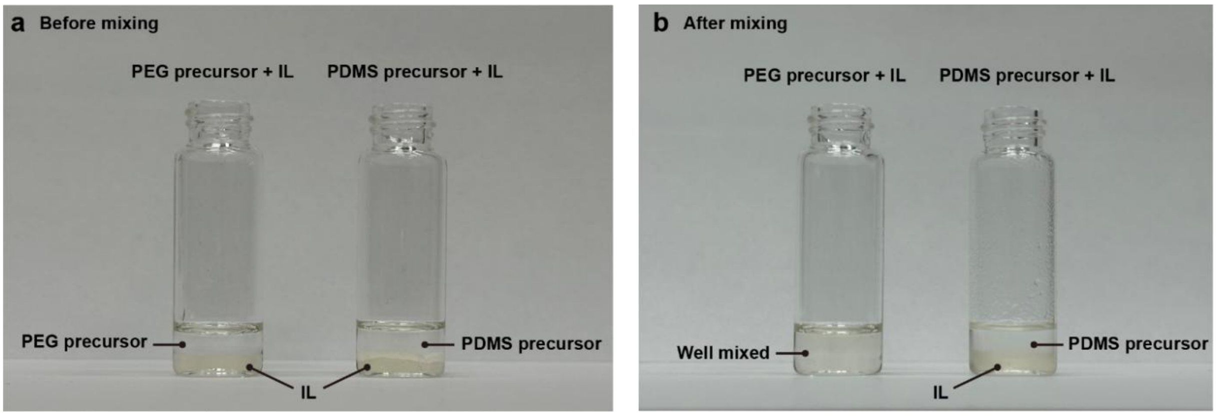

Supplementary Fig. S1. Photographs of the PEG/IL precursor and PDMS/IL precursor before and after mixing. The similar polarity of PEG precursor and ionic liquids allows for a homogeneous mixture after mixing, while the PDMS precursor and ionic liquids kept separated and cannot be mixed well.

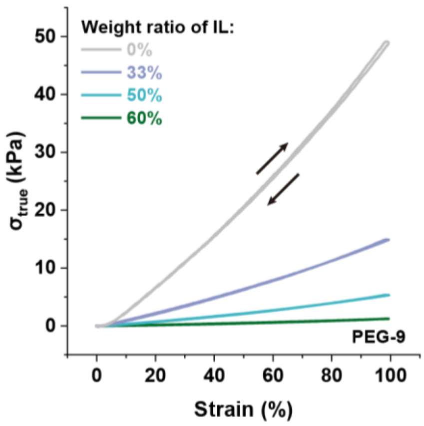

Supplementary Fig. S2. Cycling tests of PEG BBIs with different concentrations of ionic liquids at the strain of 100% showing a reversible stress-strain curve and good elasticity.

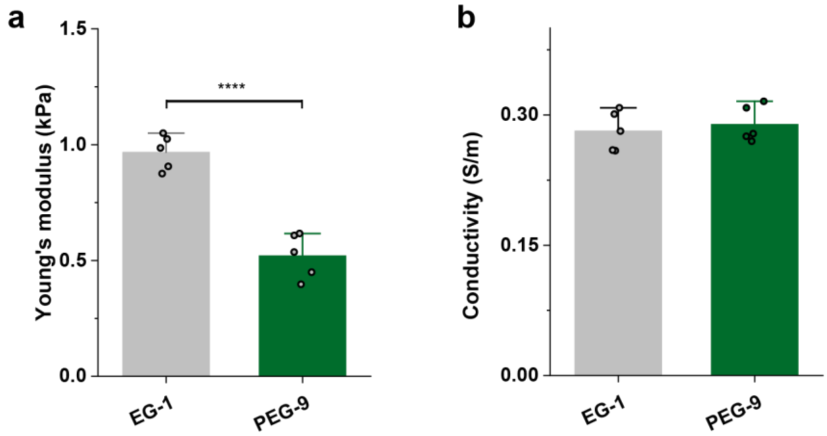

Supplementary Fig. S3. (**a**) Young's modulus and (**b**) conductivity of EG-1 ionogel and PEG-9 BBI with 70 wt% ILs. Asterisks indicate statistical significance, with **** representing $p < 0.0001$.

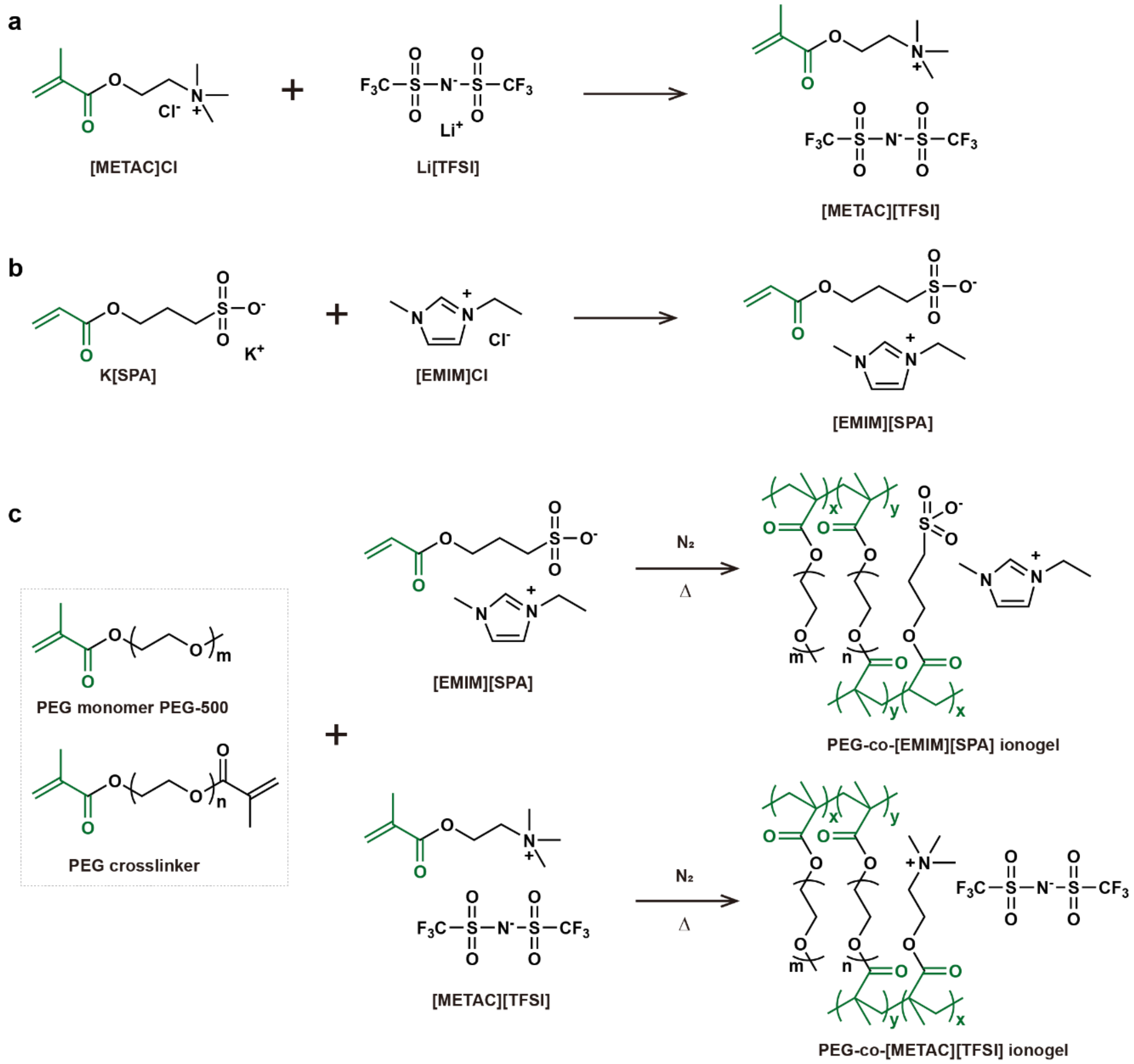

Supplementary Fig. S4. (**a**) Synthesis of [METAc][TFSI] (**b**) Synthesis of [EMIM][SPA] (**c**) Polymerization and crosslinking for PEG-co-[EMIM][SPA] ionogel and PEG-co-[METAC][TFSI] ionogel.

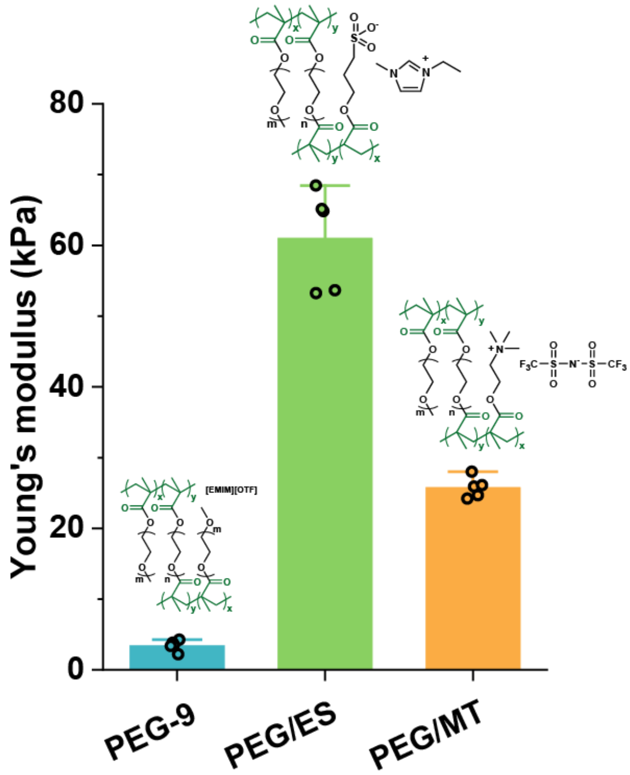

Supplementary Fig. S5. Young's modulus of PEG BBE-based ionogels prepared using [EMIM][OTf], and the reactive ionic liquids ES and MT, respectively.

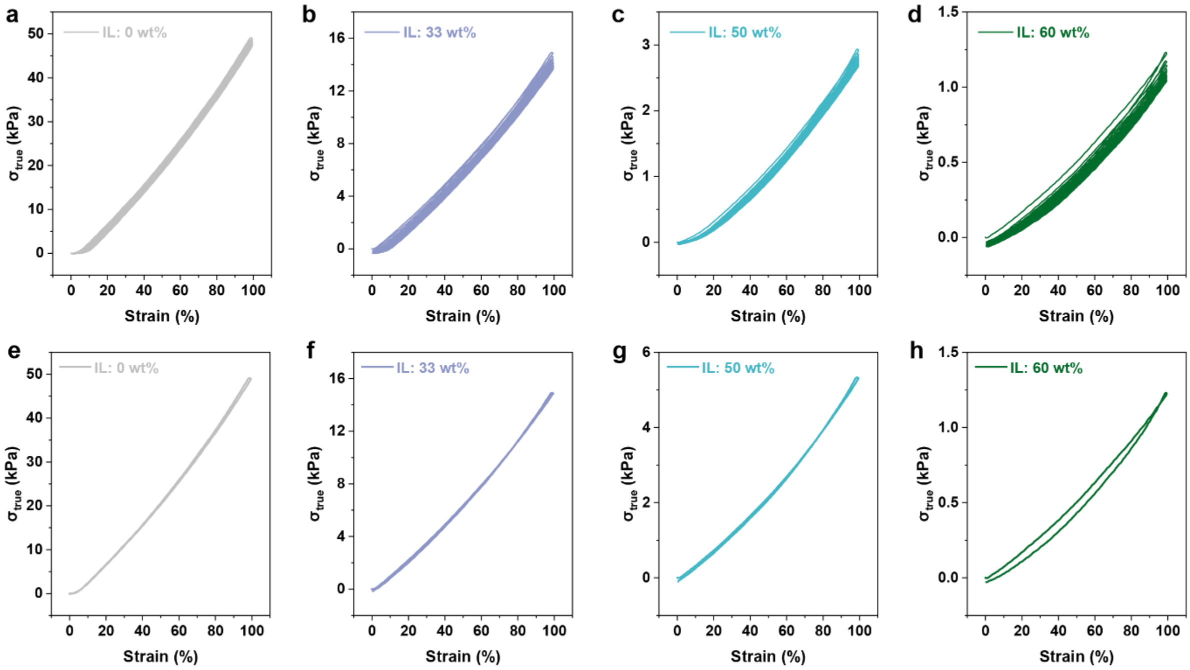

Supplementary Fig. S6. (**a**)-(**d**) Loading-unloading tests of PEG/IL bottlebrush ionogels with different ionic liquids contens [IL weight ratio: (**a**) 0%, (**b**) 33%, (**c**) 50%, and (**d**) 60%] for 10 cycles under the strain of 0 – 100%. (**e**)-(**f**) Loading-unloading tests of PEG/IL bottlebrush ionogels with different ionic liquids contens [IL weight ratio: (**c**) 0%, (**d**) 33%, (**e**) 50%, and (**f**) 60%] for 1 cycle under the strain of 0 – 100%.

Supplementary Table S1. The fitted mechanical properties of PEG/IL BBIs.

IL weight ratio	Fitted Young's modulus (E, kPa)	Engineering Young's modulus (E_{eng}, kPa)	β
0%	29.84	20.64	0.10
33%	9.46	8.58	0.11
50%	3.43	3.25	0.12
60%	1.08	1.03	0.14

The strain-stress curves were fitted by the model for bottlebrush elastomers [1,2]:

$$\sigma_{true} = \frac{E}{9}[(\varepsilon+1)^2 - (\varepsilon+1)^{-1}]\left\{1 + 2\left[1 - \frac{\beta[(\varepsilon+1)^2 - (\varepsilon+1)^{-1}]}{3}\right]\right\}$$

where σ_{true} and ε are true stress and engineering strain, and β is the strand-extension ratio and E is the structural Young's modulus, respectively. The engineering Young's modulus (E_{eng}) was determined by linear fitting the nominal stress-strain curve at the strain range of 0-10%. The Young's modulus calculated by the two methods exhibited similar levels, and the fitted Young's modulus was used for analysis. It should be noted that the fitted parameter β has a value of <0.3, lower than those of some tissues (e.g., β of fat >0.6), indicating an unmatched strain-hardening behaviour with that of tissues. The sample size is 5, and the presented values are the average calculated from results of 5 samples.

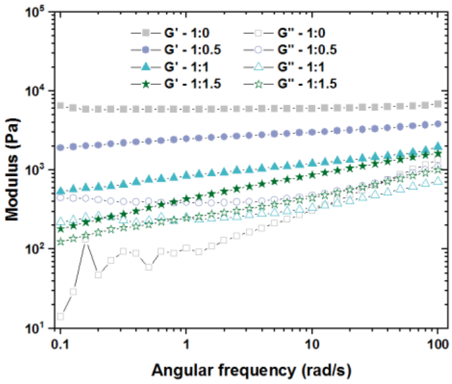

Supplementary Fig. S7. The storage modulus G' and loss modulus G'' aas a function of sweeping frequency at the strain of 1% for samples with PEG/IL ratios of 1:0 (IL: 0 wt%), 1:0.5 (IL: 33 wt%), 1:1 (IL: 50 wt%), and 1:1.5 (IL: 60 wt%). The storage modulus is nearly independent of angular frequency for pure PEG BBE. With the addition of ionic liquids, the storage modulus started to be dependent with the frequency, and the trend that the storage modulus increases with the increase of angular frequency becomes more noticeable for higher weight ratio of ionic liquids (e.g., IL: 60 wt%). The results indicate that the incorporation of ionic liquids as a viscous component within the elastic PEG bottlebrush matrix could enhance the viscoelastic behavior. This is possibly attributed to the addition of ionic liquids that affected the relaxation process of the bottlebrush networks [3,4].

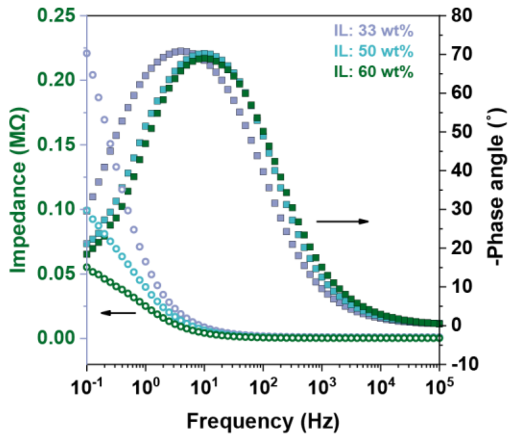

Supplementary Fig. S8. Bode plot of PEG/IL BBI with different weight ratios of ionic liquids.

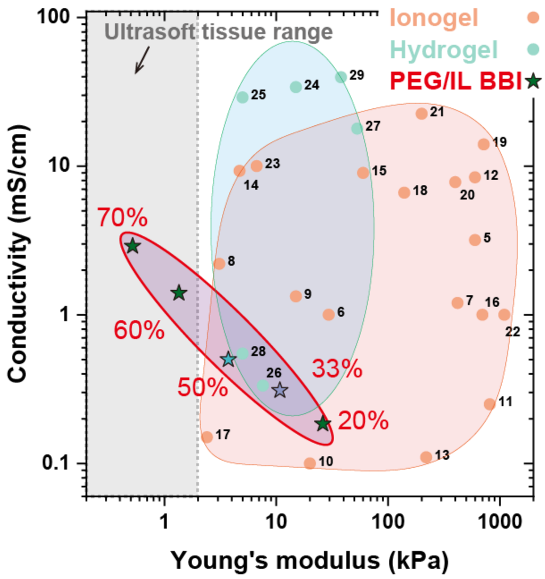

Supplementary Fig. S9. The Ashby-style plot of Young's modulus and conductivity of different ionic conductive elastomers including ionogels, hydrogels, and PEG/IL BBIs in this work, showing our PEG/IL BBI (1:1.5) is the softest ionically conductive elastomer in the graph. Here, we mainly selected soft materials with Young's modulus ranging from 1 kPa to 1 MPa, and materials with higher modulus were not included.

Supplementary Table S2. The summary of Young's modulus and conductivity of ionically conductive materials including ionogels, hydrogels, and PEG/IL BBIs in this work.

Young's modulus (kPa)	Conductivity (mS/cm)	Matrix materials	Ion species	Reference
Ionogels				
600	3.18 for ionic liquids	Sylgard 184 (dielectric materials)	1-ethylpyridinium tetrafluoroborate, -butyl-4-methylpyridinium tetra-fluoroborate	5
29.51	1	Polymeric ionic liquids with reido-pyrimidinone pendantgroups (PIL-UPy)	2-dimethyl-3-ethoxyethyl imidazolium bis(trifluoromethanesulfonyl)imide	6
420	1.2	Poly(urea-urethane)	1,2-dimethyl-3-ethoxyethyl-imidazolium bis(trifluoromethanesulfonyl)imide	7
4	2.2	Poly(acrylic acid)	1-thyl-3-methylimidazoliumethylsulfate	8
15	1.33	Poly(ethyl acrylate) (PEA)-based elastomer	1-ethyl-3-methylimidazolium bis-(trifluoromethylsulfonyl)imide	9
20	0.1	Eth-ylene glycol methyl ether acrylate (MEA) and isobornyl acrylate	1-ethyl-3-methylimidazolium bis(trifluoromethyl-sulfonyl)imide	10
815	0.25	Polymerizable [2-(methacryloy-loxy)ethyl]trimethylammonium bis(trifluoromethanesulfonyl)imide	Butyltrimethylammonium bis(trifluoromethanesulfonyl)imide	11
600	8.4	Water-dispersible polyurethane	1-ethyl-3-methylimidazolium dicyanamide	12
220	0.11	Polymerizable acryloyloxyethyltrimethylammonium bis(trifluoromethanesulfonyl)imide	Butyltrimethylammonium bis(trifluoromethanesulfonyl)imide	13

Young's modulus (kPa)	Conductivity (mS/cm)	Matrix materials	Ion species	Reference
4.7	9.3	Tetramethoxysilane and formic acid	1-Ethyl-3-methylimidazolium bis(trifluoromethylsulfonyl)imide	14
60	9	Poly(vinylidene fluoride-cohexafluoropropylene) (PVdF-HFP)	1-ethyl-3-methylimidazolium tetracyanoborate	15
700	1	Poly(vinylidenefluoride-co-hexafluoropropylene) (P(VDF-co-HFP)) and poly(methyl methacrylate-co-butylmetha-crylate) (P(MMA-co-BMA)) elastomer	1-Ethyl-3-methylimidazolium bis(trifluoromethylsulfonyl)imide	16
2.4	0.15	Butyl acrylate	Bis(trifluoromethylsulfonyl imide)	17
140	6.63 for ionic liquids	Poly(tert-butyl styrene-block-(4-hydroxystyrene-random-methyl acrylate)) and poly(tert-butyl styrene-block-(2-vinyl pyridine-random-methyl acrylate))	1-Ethyl-3-methylimidazolium bis(trifluoromethylsulfonyl)imide	18
720	14	Polyurethane	1-propyl-3-methyl-imidazolium bis(trifluoromethyl-sulfonyl) imide	19
400	7.8	Cellulose nanocrystals (CNCs) grafted with poly(ionic liquid)s	1-ethyl-3-methylimidazolium bis(trifluoromethylsulfonyl)imide	20
200	22.5	Poly(urethane-urea)	1-Ethyl-3-methylimidazolium dicyanamide	21
1100	1	Microcrystalline cellulose	1-ethyl-3-methylimidazolium acetate	22
6.7	10	Poly(acrylic acid)	1-ethyl-3-methylimidazolium ethylsulfate	23
Hydrogels				
15	34	Polyvinyl alcohol (PVA)	NaCl	24
5	29	Polyacrylamide	NaCl	25

Young's modulus (kPa)	Conductivity (mS/cm)	Matrix materials	Ion species	Reference
7.6	0.334	Poly-ligo(ethylene glycol)methacrylate	NaCl	[26]
53	17.9	Copolymerized lauryl methacrylate and acrylamide	LiCl	[27]
5	0.548	[2-(Methacryloyloxy) ethyl]dimethyl-(3-sulfopropyl) ammonium hy-droxide hydrogels	[2-(Methacryloyloxy) ethyl]dimethyl-(3-sulfopropyl) ammonium hy-droxide	[28]
38	39.6	Acrylamide and amine-functionalized monomer based hydrogels	LiCl	[29]
PEG/IL BBI				
10.78	0.31	PEG-based BBI	[EMIM][OTF]	This work
3.73	0.5	PEG-based BBI	[EMIM][OTF]	
1.35	1.4	PEG-based BBI	[EMIM][OTF]	

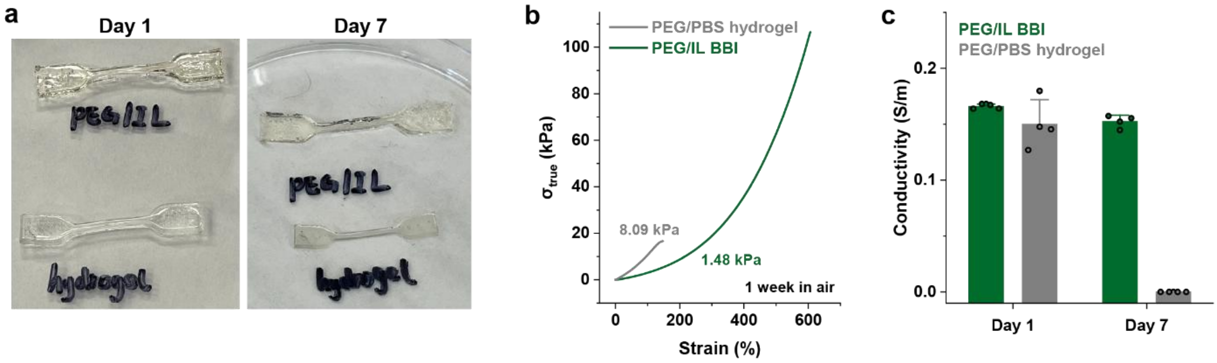

Supplementary Fig. S10. The (**a**) images, (**b**) tensile tests, and (**c**) conductivity measurements of PEG/IL BBI and PEG/PBS hydrogels after exposed in air for 1 week. Compared to the PEG/IL bottlebrush ionogel, the PEG/PBS hydrogel experienced a decay of conductivity, stretchability, and softness due to the loss of water. These results show superior stability of PEG/IL BBI compared to PEG/PBS hydrogels.

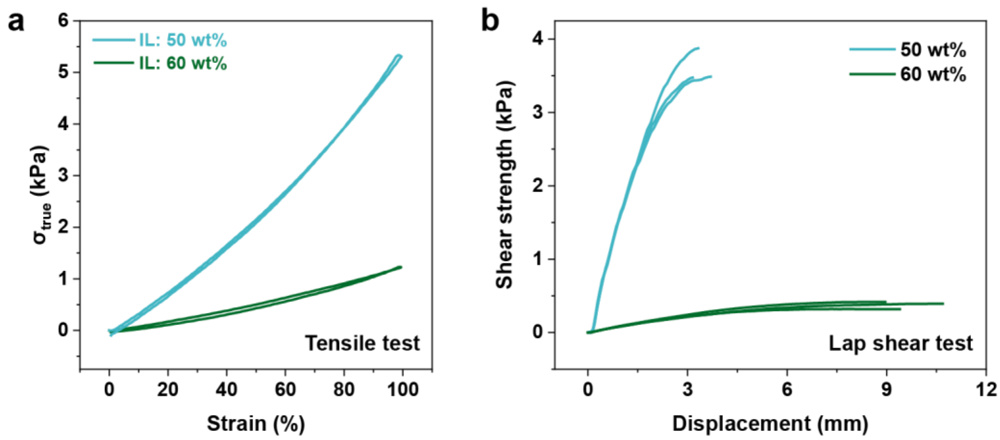

Supplementary Fig. S11. The results of (**a**) tensile tests and (**b**) lap shear tests for samples with IL weight ratios of 50% and 60%. One can see that both the tensile strength and shear strength of samples with 60 wt% IL are lower than those samples with 50 wt% IL, indicating that the decline of shear strength of softer sample is possibly due to the its lower bulk strength than that of “harder” sample.

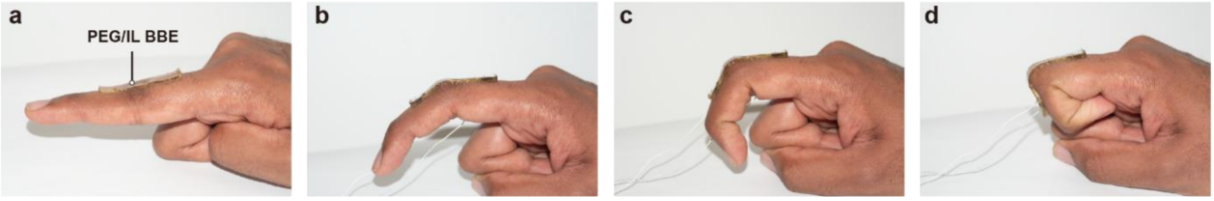

Supplementary Fig. S12. Photographs showing PEG/IL BBI can easily attach to skin and maintain the conformal contact when the finger was bending.

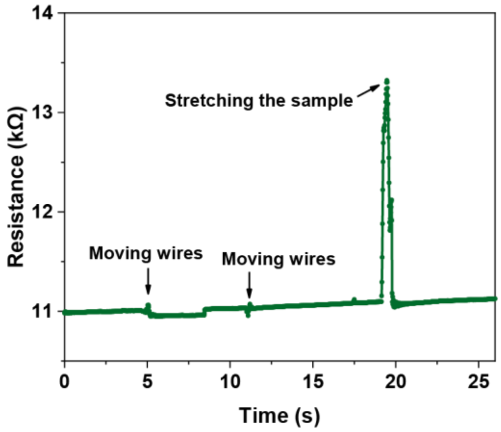

Supplementary Fig. S13. The much smaller resistance change from moving wires compared to that by stretching the sample shows the negligible electrical effect of contact at the wire-Ag/EGaIn interface. The stretching strain is 2%.

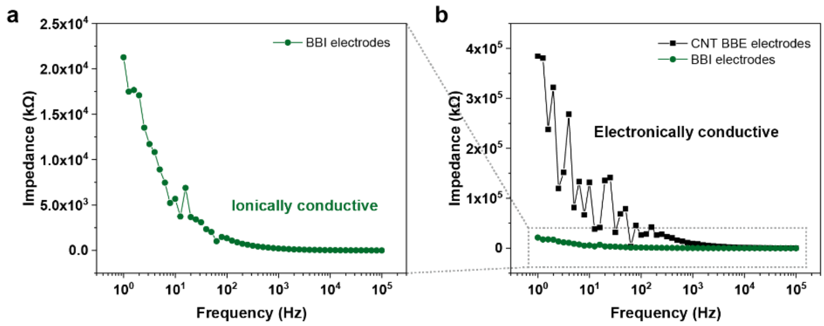

Supplementary Fig. S14. (**a-b**) Skin impedance measurements using ionically conductive PEG/IL BBI electrodes and electronically conductive CNT BBE electrodes.

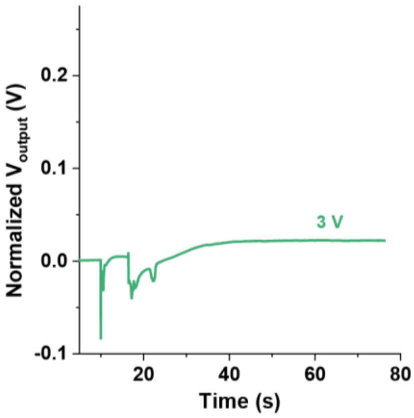

Supplementary Fig. S15. Normalized output voltage measured from the Venus trap with the applied DC voltage of 3 V.

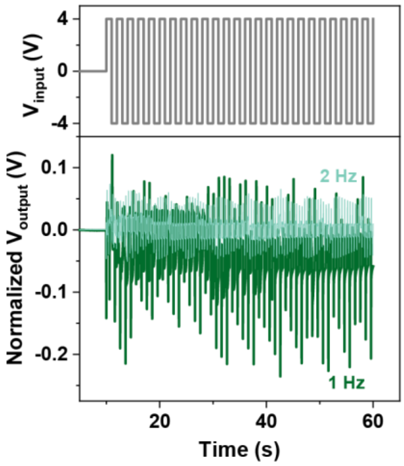

Supplementary Fig. S16. The recorded signal response from the Venus flytrap stimulated by AC voltage inputs with the amplitude of 4 V and frequencies of 1 Hz and 2 Hz, respectively.

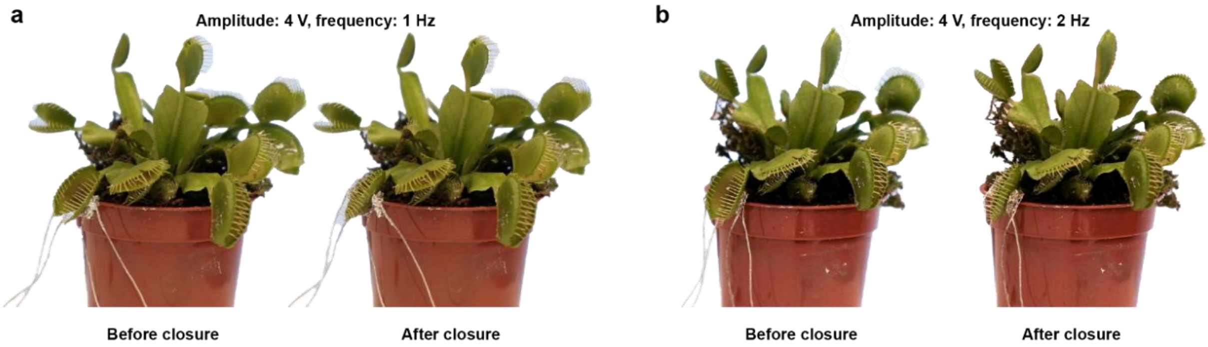

Supplementary Fig. S17. (**a**) Photographs showing the lobe closure of the Venus flytrap stimulated by an AC voltage input with the amplitude of 4 V and frequencies of 1 Hz. The response time was 1.3 s. (**b**) Photographs showing the lobe closure of the Venus flytrap stimulated by an AC voltage input with the amplitude of 4 V and frequencies of 2 Hz. The response time was 1 s.

Supplementary Table S3. Comparison of different conductive bottlebrush elastomers.

Materials	Preparation method	Applications	Young's modulus, Stretchability, Conductivity			Charge carriers	Reference
Poly(4-methylcaprolactone) BBE/carbon nanotubes	Ring-opening polymerization; bottlebrush polymers need to be self-synthesized	Resistor	66 kPa	/	10^{-2} S/m	Electrons	[30]
PDMS BBE/carbon nanotubes	Free radical polymerization; all materials are commercially available	Force sensor for human-machine interface	2.98 kPa	>100%	2.06 S/m	Electrons	[31]
PEG/IL bottlebrush ionogels	Free radical polymerization; all materials are commercially available	Wearable electrodes for plants and human	0.52 kPa to 9.46 kPa	>100%	0.03 S/m to 0.29 S/m	Ions	This work

References

(1) Vatankhah-Varnosfaderani, M.; Daniel, W. F. M.; Everhart, M. H.; Pandya, A. A.; Liang, H.; Matyjaszewski, K.; Dobrynin, A. V.; Sheiko, S. S. Mimicking Biological Stress–Strain Behaviour with Synthetic Elastomers. *Nature* **2017**, *549* (7673), 497–501. https://doi.org/10.1038/nature23673.

(2) Keith, A. N.; Vatankhah-Varnosfaderani, M.; Clair, C.; Fahimipour, F.; Dashtimoghadam, E.; Lallam, A.; Sztucki, M.; Ivanov, D. A.; Liang, H.; Dobrynin, A. V.; Sheiko, S. S. Bottlebrush Bridge between Soft Gels and Firm Tissues. *ACS Cent. Sci.* **2020**, *6* (3), 413–419. https://doi.org/10.1021/acscentsci.9b01216.

(3) Cao, Z.; Daniel, W. F. M.; Vatankhah-Varnosfaderani, M.; Sheiko, S. S.; Dobrynin, A. V. Dynamics of Bottlebrush Networks. *Macromolecules* **2016**, *49* (20), 8009–8017. https://doi.org/10.1021/acs.macromol.6b01358.

(4) Barkoula, N. M.; Alcock, B.; Cabrera, N. O.; Peijs, T. An Investigation on the Rheology, Morphology, Thermal and Mechanical Properties of Recycled Poly (Ethylene Terephthalate) Reinforced With Modified Short Glass Fibers. *Polym. Compos.* **2009**, *30* (7), 993–999. https://doi.org/10.1002/pc.

(5) Su, J.; Yu, L.; Skov, A. L. Remarkable Improvement of the Electro-Mechanical Properties of Polydimethylsiloxane Elastomers through the Combined Usage of Glycerol and Pyridinium-Based Ionic Liquids. *Polym. Technol. Mater.* **2020**, *59* (3), 271–281. https://doi.org/10.1080/25740881.2019.1625398.

(6) Guo, P.; Su, A.; Wei, Y.; Liu, X.; Li, Y.; Guo, F.; Li, J.; Hu, Z.; Sun, J. Healable, Highly Conductive, Flexible, and Nonflammable Supramolecular Ionogel Electrolytes for Lithium-Ion Batteries. *ACS Appl. Mater. Interfaces* **2019**, *11* (21), 19413–19420. https://doi.org/10.1021/acsami.9b02182.

(7) Li, T.; Wang, Y.; Li, S.; Liu, X.; Sun, J. Mechanically Robust, Elastic, and Healable Ionogels for Highly Sensitive Ultra-Durable Ionic Skins. *Adv. Mater.* **2020**, *32* (32), 1–7. https://doi.org/10.1002/adma.202002706.

(8) Chen, B.; Lu, J. J.; Yang, C. H.; Yang, J. H.; Zhou, J.; Chen, Y. M.; Suo, Z. Highly Stretchable and Transparent Ionogels as Nonvolatile Conductors for Dielectric Elastomer Transducers. *ACS Appl. Mater. Interfaces* **2014**, *6* (10), 7840–7845. https://doi.org/10.1021/am501130t.

(9) Cao, Z.; Liu, H.; Jiang, L. Transparent, Mechanically Robust, and Ultrastable Ionogels Enabled by Hydrogen Bonding between Elastomers and Ionic Liquids. *Mater. Horizons* **2020**, *7* (3), 912–918. https://doi.org/10.1039/c9mh01699f.

(10) Yiming, B.; Guo, X.; Ali, N.; Zhang, N.; Zhang, X.; Han, Z.; Lu, Y.; Wu, Z.; Fan, X.; Jia, Z.; Qu, S. Ambiently and Mechanically Stable Ionogels for Soft Ionotronics. *Adv. Funct. Mater.* **2021**, *31* (33), 1–11. https://doi.org/10.1002/adfm.202102773.

(11) Yu, Z.; Wu, P. Underwater Communication and Optical Camouflage Ionogels. *Adv. Mater.* **2021**, *33* (24), 1–10. https://doi.org/10.1002/adma.202008479.

(12) Fang, Y.; Cheng, H.; He, H.; Wang, S.; Li, J.; Yue, S.; Zhang, L.; Du, Z.; Ouyang, J. Stretchable and Transparent Ionogels with High Thermoelectric Properties. *Adv. Funct. Mater.* **2020**, *30* (51), 1–8. https://doi.org/10.1002/adfm.202004699.

(13) Yu, Z.; Wu, P. Water-Resistant Ionogel Electrode with Tailorable Mechanical Properties for Aquatic Ambulatory Physiological Signal Monitoring. *Adv. Funct. Mater.* **2021**, *31* (51), 1–7. https://doi.org/10.1002/adfm.202107226.

(14) Horowitz, A. I.; Panzer, M. J. High-Performance, Mechanically Compliant Silica-Based Ionogels for Electrical Energy Storage Applications. *J. Mater. Chem.* **2012**, *22* (32), 16534–16539. https://doi.org/10.1039/c2jm33496h.

(15) Pandey, G. P.; Hashmi, S. A. Ionic Liquid 1-Ethyl-3-Methylimidazolium Tetracyanoborate-Based Gel Polymer Electrolyte for Electrochemical Capacitors. *J. Mater. Chem. A* **2013**, *1* (10), 3372–3378. https://doi.org/10.1039/c2ta01347a.

(16) Lan, J.; Li, Y.; Yan, B.; Yin, C.; Ran, R.; Shi, L. Y. Transparent Stretchable Dual-Network Ionogel with Temperature Tolerance for High-Performance Flexible Strain Sensors. *ACS Appl. Mater. Interfaces* **2020**, *12* (33), 37597–37606. https://doi.org/10.1021/acsami.0c10495.

(17) Sun, J.; Yuan, Y.; Lu, G.; Li, L.; Zhu, X.; Nie, J. A Transparent, Stretchable, Stable, Self-Adhesive Ionogel-Based Strain Sensor for Human Motion Monitoring. *J. Mater. Chem. C* **2019**, *7* (36), 11244–11250. https://doi.org/10.1039/c9tc03797g.

(18) Cho, K. G.; An, S.; Cho, D. H.; Kim, J. H.; Nam, J.; Kim, M.; Lee, K. H. Block Copolymer-Based Supramolecular Ionogels for Accurate On-Skin Motion Monitoring. *Adv. Funct. Mater.* **2021**, *31* (36), 1–11. https://doi.org/10.1002/adfm.202102386.

(19) Xu, J.; Wang, H.; Du, X.; Cheng, X.; Du, Z.; Wang, H. Self-Healing, Anti-Freezing and Highly Stretchable Polyurethane Ionogel as Ionic Skin for Wireless Strain Sensing. *Chem. Eng. J.* **2021**, *426* (May), 130724. https://doi.org/10.1016/j.cej.2021.130724.

(20) Lee, H.; Erwin, A.; Buxton, M. L.; Kim, M.; Stryutsky, A. V.; Shevchenko, V. V.; Sokolov, A. P.; Tsukruk, V. V. Shape Persistent, Highly Conductive Ionogels from Ionic Liquids Reinforced with Cellulose Nanocrystal Network. *Adv. Funct. Mater.* **2021**, *31* (38), 1–14. https://doi.org/10.1002/adfm.202103083.

(21) Chen, L.; Guo, M. Highly Transparent, Stretchable, and Conductive Supramolecular Ionogels Integrated with Three-Dimensional Printable, Adhesive, Healable, and Recyclable Character. *ACS Appl. Mater. Interfaces* **2021**. https://doi.org/10.1021/acsami.1c04255.

(22) Song, H.; Luo, Z.; Zhao, H.; Luo, S.; Wu, X.; Gao, J.; Wang, Z. High Tensile Strength and High Ionic Conductivity Bionanocomposite Ionogels Prepared by Gelation of Cellulose/Ionic Liquid Solutions with Nano-Silica. *RSC Adv.* **2013**, *3* (29), 11665–11675. https://doi.org/10.1039/c3ra40387d.

(23) Zhang, L. M.; He, Y.; Cheng, S.; Sheng, H.; Dai, K.; Zheng, W. J.; Wang, M. X.; Chen, Z. S.; Chen, Y. M.; Suo, Z. Self-Healing, Adhesive, and Highly Stretchable Ionogel as a Strain Sensor for Extremely Large Deformation. *Small* **2019**, *15* (21), 1–8. https://doi.org/10.1002/smll.201804651.

(24) Zhou, Y.; Wan, C.; Yang, Y.; Yang, H.; Wang, S.; Dai, Z.; Ji, K.; Jiang, H.; Chen, X.; Long, Y. Highly Stretchable, Elastic, and Ionic Conductive Hydrogel for Artificial Soft Electronics. *Adv. Funct. Mater.* **2019**, *29* (1), 1–8. https://doi.org/10.1002/adfm.201806220.

(25) Odent, J.; Wallin, T. J.; Pan, W.; Kruemplestaedter, K.; Shepherd, R. F.; Giannelis, E. P. Highly Elastic, Transparent, and Conductive 3D-Printed Ionic Composite Hydrogels. *Adv. Funct. Mater.* **2017**, *27* (33), 1–10. https://doi.org/10.1002/adfm.201701807.

(26) Wei, P.; Chen, T.; Chen, G.; Liu, H.; Mugaanire, I. T.; Hou, K.; Zhu, M. Conductive Self-Healing Nanocomposite Hydrogel Skin Sensors with Antifreezing and Thermoresponsive Properties. *ACS Appl. Mater. Interfaces* **2020**, *12* (2), 3068–3079. https://doi.org/10.1021/acsami.9b20254.

(27) Xia, S.; Zhang, Q.; Song, S.; Duan, L.; Gao, G. Bioinspired Dynamic Cross-Linking Hydrogel Sensors with Skin-like Strain and Pressure Sensing Behaviors. *Chem. Mater.* **2019**, *31* (22), 9522–9531. https://doi.org/10.1021/acs.chemmater.9b03919.

(28) Wang, L.; Gao, G.; Zhou, Y.; Xu, T.; Chen, J.; Wang, R.; Zhang, R.; Fu, J. Tough, Adhesive, Self-Healable, and Transparent Ionically Conductive Zwitterionic Nanocomposite Hydrogels as Skin Strain Sensors. *ACS Appl. Mater. Interfaces* **2019**, *11* (3), 3506–3515. https://doi.org/10.1021/acsami.8b20755.

(29) Wu, M.; Chen, J.; Ma, Y.; Yan, B.; Pan, M.; Peng, Q.; Wang, W.; Han, L.; Liu, J.; Zeng, H. Ultra Elastic, Stretchable, Self-Healing Conductive Hydrogels with Tunable Optical Properties for Highly Sensitive Soft Electronic Sensors. *J. Mater. Chem. A* **2020**, *8* (46), 24718–24733. https://doi.org/10.1039/d0ta09735g.

(30) Self, J. L.; Reynolds, V. G.; Blankenship, J.; Mee, E.; Guo, J.; Albanese, K.; Xie, R.; Hawker, C. J.; de Alaniz, J. R.; Chabinyc, M. L.; Bates, C. M. Carbon Nanotube Composites with Bottlebrush Elastomers for Compliant Electrodes. *ACS Polym. Au* **2021**. https://doi.org/10.1021/acspolymersau.1c00034.

(31) Xu, P.; Wang, S.; Lin, A.; Min, H.-K.; Zhou, Z.; Dou, W.; Sun, Y.; Huang, X.; Tran, H.; Liu, X. Conductive and Elastic Bottlebrush Elastomers for Ultrasoft Electronics. *Nat. Commun.* **2023**, *14* (623). https://doi.org/10.1038/s41467-023-36214-8.